Angle Droop versus Frequency Droop in a Voltage Source Converter Based Autonomous Microgrid

Ritwik Majumder, *Student Member, IEEE*, Arindam Ghosh, *Fellow, IEEE*
Gerard Ledwich, *Senior Member, IEEE* and Firuz Zare, *Senior Member, IEEE*

ABSTRACT: This paper compares the performance of angle and frequency droops in an autonomous microgrid that only contains voltage source converter (VSC) interfaced distributed generators (DGs). As a VSC can instantaneously change output voltage waveform, power sharing in a microgrid is possible by controlling the output voltage angle of the DGs through droop. The angle droop is able to provide proper load sharing among the DGs without a significant steady state frequency drop in the system. It is shown that the frequency variation with the frequency droop controller is significantly higher than that with the angle droop controller. The angle droop controller is derived from DC load flow. Both the angle and frequency droop controllers are designed through eigenvalue analysis. The performance of these two controllers is then performed through PSCAD simulations.

I. Introduction

MICROGRID CAN generally be viewed as a cluster of distributed generators connected to the main utility grid, usually through voltage-source-converter (VSC) based interfaces. Concerning the interfacing of the distributed resources to the microgrid, it is important to achieve a proper load sharing amongst them. A load sharing with minimal communication is the best in the distribution level as the network is complex, can be reconfigured and may span over a large area. The most common method is the use of droop characteristics. The use of local signals as feedback to control the converters is desirable, since in a real system, the distance between the converters may make an inter communication impractical. Parallel converters have been controlled to deliver desired real and reactive power to the system. With this in mind, this paper proposes a configuration that is suitable for supplying electrical power of high quality to the microgrid, specifically when it is being supplied through controlled VSCs.

The real and reactive power sharing can be achieved by controlling two independent quantities – the system frequency and the fundamental voltage magnitude [1-5]. In these papers, the frequency droop is used to share the real power. The DGs have the potential to deliver reliable power when their locations are strategically planned. However, for large scale application of DGs, the commercial and regulatory challenges have to be considered before their benefits can be realized [6]. One of the most significant aspects is the change in system frequency. As discussed in [1-5], the real power output of the DGs is controlled by dropping the system frequency. Depending on the stiffness of the power-frequency curve, the steady state frequency will change with the changes in system loads.

R. Majumder, A. Ghosh, G. Ledwich and F. Zare are with the School of Engineering Systems, Queensland University of Technology, Brisbane, Qld 4001, Australia.

Since it is not desirable to operate the system in a much lower frequency, a complimentary frequency restoration strategy is proposed in [4]. The frequency may then be restored to its nominal value by a slower outer control loop. The reference powers of the DGs are modified to restore the frequency which is equivalent to shifting the power-frequency curve vertically. The process can be controlled in a slow, coordinated manner by a master controller, using a slow communication channel between the inverters [4]. In conversational frequency droop the frequency deviation signal is used to set the power output of the converter. The limitations of the use of frequency deviation alone have been established for many years [7]. Nevertheless, the conventional droop method remains several drawbacks that limit its application area, such as: slow transient response, frequency and amplitude deviations, unbalance harmonic current sharing, and high dependency on the inverter output-impedance [8]. Some times high frequency signals are injected to overcome the unbalance reactive power flow. Since the power balance and the system stability rely on these signals, the application of such signal increases system complexity and reduces reliability.

In this paper it is shown that in a microgrid with frequency droop, the variation of frequency with normal load changes tends to be much higher than system grid frequency variation. Trying to correct this using low droop coefficient may lead to large variations in the frequency.

As a VSC can instantaneously change its output voltage waveform, power sharing in a microgrid is possible by controlling the output voltage angle of the DGs through droop. A simple microgrid system with two DG and one load is considered for establishing the advantage of angle droop. First, the load sharing with angle droop is derived using the DC load flow method. It is shown that it is possible to share power proportional to their rating among the DGs by dropping the output voltage angles. To compare the performance of the angle droop controller with frequency droop controller, both the controllers are designed for the same system mentioned above. The controllers are designed ensuring same stability margin. The load conductance is chosen as the integral of a Gaussian white noise source with zero mean and standard deviation of 0.01 Mho. It is shown that the standard deviation of frequency with angle droop is much smaller than standard deviation of frequency with frequency droop. The restoration of frequency is not required in angle droop as the steady state frequency drop is much less. However for the measurement of angles with respect to a common reference, GPS communications is needed with angle droop control. The efficacy of the proposed angle droop controller is then validated in a microgrid with multiple DGs and loads through simulation for various operating conditions using PSCAD.

II. Load Sharing with Angle Droop

The angle droop control strategy is applied to all the DGs in the system. It is assumed that the total power demand in the microgrid can be supplied by the DGs such that no load shedding is required. The output voltages of the converters are controlled to share the load proportional to the rating of the DGs. As an output inductance is connected to each of the VSCs, the real and reactive power injection from the DG source to the microgrid can be controlled by changing voltage magnitude and its angle [1-4]. Fig. 1 shows the power flow from a DG to the microgrid where the rms values of the voltages and current are shown and the output impedance is denoted by jX_f. It is to be noted that real and reactive power (P and Q) shown in the figure are the average values.

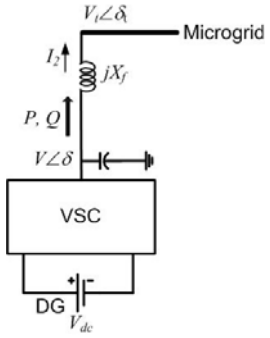

Fig. 1. DG connection to microgrid.

A. Angle Droop Control and Power Sharing

Let the instantaneous real power be denoted by p and the reactive power be denoted by q. Then these powers, from the DG to the microgrid, can be calculated as

$$p = \frac{V \times V_t \sin(\delta - \delta_t)}{X_f}$$
$$q = \frac{V^2 - V \times V_t \cos(\delta - \delta_t)}{X_f} \quad (1)$$

These instantaneous powers are passed through low pass filter to obtain the average real and reactive power P and Q. It is to be noted that the VSC does not have any direct control over the microgrid voltage at the bus $V_t\angle\delta_t$ (see Fig. 1). Hence from (1), it is clear that if the angle difference ($\delta - \delta_t$) is small, the real power can be controlled by controlling δ, while the reactive power can be controlled by controlling voltage magnitude. Thus the power requirement can be distributed among the DGs, similar to conventional droop by dropping the voltage magnitude and angle as

$$\delta = \delta_{rated} - m \times (P_{rated} - P)$$
$$V = V_{rated} - n \times (Q_{rated} - Q) \quad (2)$$

where V_{rated} and δ_{rated} are the rated voltage magnitude and angle respectively of the DG, when it is supplying the load to its rated power levels of P_{rated} and Q_{rated}. The coefficients m and n respectively indicate the voltage angle drop vis-à-vis the real power output and the voltage magnitude drop vis-à-vis the reactive power output. These values are chosen to meet the voltage regulation requirement in the microgrid.

To derive the power sharing with angle droop, a simple system with two machines and a load is considered as shown in Fig. 2. The voltages and the power flow are indicated in the figure. Applying DC load flow with all the necessary assumptions we get,

$$\delta_1 - \delta = (X_1 + X_{L1})P_1$$
$$\delta_2 - \delta = (X_2 + X_{L2})P_2 \quad (3)$$

where $X_1 = \omega L_1/(V_1 V)$, $X_{L1} = \omega L_{Line1}/(V_1 V)$, $X_2 = \omega L_2/(V_2 V)$ and $X_{L2} = \omega L_{Line2}/(V_2 V)$.

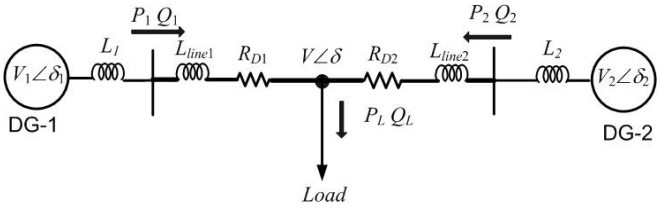

Fig. 2. DG connection to microgrid.

The angle droop equations of the DGs are given by

$$\delta_1 = \delta_{1rated} - m_1 \times (P_{1rated} - P_1)$$
$$\delta_2 = \delta_{2rated} - m_2 \times (P_{2rated} - P_2) \quad (4)$$

The offsets in the angle droop are taken such that when DG output power is zero, the DG source angle is zero. Hence the rated droop angles are taken as $\delta_{1rated} = m_1 P_{1rated}$ and $\delta_{2rated} = m_2 P_{2rated}$. Then from (4) we get

$$\delta_1 - \delta_2 = m_1 P_1 - m_2 P_2 \quad (5)$$

Similarly from (3) we get

$$\delta_1 - \delta_2 = (X_1 + X_{L1})P_1 - (X_2 + X_{L2})P_2 \quad (6)$$

Assuming the system to be lossless, we can find from Fig. 2 that $P_2 = P_L - P_1$ and substituting this (5) and (6) we get,

$$(X_1 + X_{L1})P_1 - (X_2 + X_{L2})(P_L - P_1) = m_1 P_1 - m_2 (P_L - P_1)$$
$$\Rightarrow P_1 = \frac{X_2 + X_{L2} + m_2}{X_2 + X_{L2} + m_2 + X_1 + X_{L1} + m_1} \quad (7)$$

Similarly P_2 can be calculated as

$$P_2 = \frac{X_1 + X_{L1} + m_1}{X_2 + X_{L2} + m_2 + X_1 + X_{L1} + m_1} \quad (8)$$

From (7) and (8), the ratio of the output power is calculated as,

$$\frac{P_1}{P_2} = \frac{X_2 + X_{L2} + m_2}{X_1 + X_{L1} + m_1} \quad (9)$$

It is to be noted that the value of X_1 and X_2 are very small compared to the value of m_1 and m_2. Moreover if the microgrid line is considered to be mainly resistive with low line inductance and the DG output inductance is much larger, we can write

$$m_1 >> X_1 >> X_{L1} \text{ and } m_2 >> X_2 >> X_{L2}$$

Therefore from (9), it is evident that the droop coefficients play the dominant role in the power sharing. Since the droop coefficients are taken as inversely proportional to the DG rating, from (9) we can write

$$\frac{P_1}{P_2} \approx \frac{m_2}{m_1} = \frac{P_{1rated}}{P_{2rated}} \tag{10}$$

The error is further reduced by taking the output inductance (L_1 and L_2) of the DGs inversely proportional to power rating of the DGs. If the microgrid line is inductive in nature and of high value, then a knowledge about the network is needed to minimize the error by choosing the DG output inductance such that

$$\frac{X_1 + X_{line1}}{X_2 + X_{line2}} = \frac{P_{2rated}}{P_{1rated}}$$

B. Frequency Droop Control and Power Sharing

The frequency droop controller share power as described in [4], where the system frequency and output voltage of the converter are controlled as,

$$\begin{aligned} \omega &= \omega_{rated} - m_\omega \times (P_{rated} - P) \\ V &= V_{rated} - n_\omega \times (Q_{rated} - Q) \end{aligned} \tag{11}$$

III. Converter Structure and Control

DG-1 is assumed to be an ideal dc voltage source supplying a voltage of V_{dc1} to the VSC. The converter contains three H-bridges. The outputs of each H-bridge are connected to single-phase transformers and the three transformers are connected in Y. The VSC is controlled under closed-loop feedback. Consider the equivalent circuit of one phase of the converter as shown in Fig. 3. In this, $u \cdot V_{dc1}$ represents the converter output voltage, where u is the switching function that can take on values ± 1. The resistance R_f represents the switching and transformer losses, while the inductance L_f represents the leakage reactance of the transformers. The filter capacitor C_f is connected to the output of the transformers to bypass switching harmonics, while L_{G1} represents the output inductance of the DG source. The converter structures of all the single phase DG sources are same.

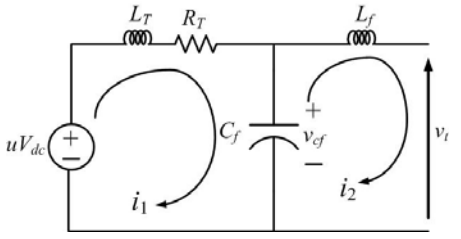

Fig. 3. Single-phase equivalent circuit of VSC.

The main aim of the converter control is to generate u. A state feedback controller used for the VSC needs three states, converter output voltage (voltage across the capacitor v_{cf}), output current and the filter current. Since V and δ are obtained from the droop equation (1), the reference for the capacitor voltage and current are given by

$$v_{cfref} = V\cos(\omega t + \delta) \tag{12}$$

$$i_{cfref} = V\omega C_f \sin(\omega t + \delta) \tag{13}$$

The reference for the current i_2 can be calculated as

$$i_{2ref} = \frac{v_{cf} - v_t}{jX_f} \tag{14}$$

The above equation will need a phase shifter for the calculation of the instantaneous current reference. This may not be desirable. Hence the measured values of the average real and reactive power output of the VSC can be used to find the magnitude and phase angle of the reference rms current. From Fig. 1, it can be seen that

$$\left|I_{2ref}\right| = \frac{\sqrt{P^2 + Q^2}}{V_{cf}} \text{ and } \angle I_{2ref} = \delta - \tan^{-1}(Q/P)$$

where $V_{cf} = V$. Hence the current reference can be given as

$$i_{2ref} = \left|I_{2ref}\right| \cos(\omega t + \angle I_{2ref}) \tag{15}$$

The state feedback and the switching control laws are given as

$$u_c(k) = K\left[x^*(k) - x(k)\right] \tag{16}$$

$$\begin{aligned} &\text{If } u_c > h \text{ then } u = +1 \\ &\text{elseif } u_c < -h \text{ then } u = -1 \end{aligned} \tag{17}$$

where h is a small number. In (16), K is the feedback gain matrix and x^* is the reference state vector. In this paper, this gain matrix is designed using LQR method. How the references are set for either of the controller will be discussed in the next section.

IV. Converter Model and Controller Design

Both the angle droop and frequency droop controllers are designed for the system shown in Fig. 2 ensuring the same stability margin The stability of the microgrid is studied through a state space model. The system equations are nonlinear and thus they are linearized to perform eigenvalue analysis. The linear quantities are denoted by the prefix Δ. The measured real and reactive power output (ΔP, ΔQ) of converter is fed to the droop controller, while voltage reference (Δv_{cfref}, $\Delta \delta_{ref}$), set by droop controller, is fed back to the converter. The circuit equations are decomposed into an equivalent D-Q reference frame. Each of the DG sources outputs current to the network, which is converter output current (Δi_{2D}, Δi_{2Q}). The input to each DG is the network voltage (Δv_{tD}, Δv_{tQ}). The state space equations of the each DG-VSC are derived separately in a modular fashion. Since the variation in the network frequency is considered very small, the network can be assumed to be completely described by the nodal admittance equation [9]. It is considered that state-less impedance model of the network may be inadequate for combining with the full-order inverter model, which includes high fre-

quency modes [10]. For this reason a dynamic (state-space) model of the network is formed on the common reference frame. The DGs are then connected to the network to get the entire microgrid model, which is not shown in this paper. The outline of the linearized model of the converter is given below.

A. Converter Model

From equivalent circuit shown in Fig. 3, the following equations are obtained for each of the phases of the three-phase system

$$\frac{di_1}{dt} = -\frac{R_T}{L_T} i_1 + \frac{\left(-v_{cf} + u.V_{dc}\right)}{L_T} \tag{18}$$

$$\frac{dv_{cf}}{dt} = \frac{\left(i_1 - i_2\right)}{C_f} \tag{19}$$

$$v_{cf} - v_t = L_f \frac{di_2}{dt} \tag{20}$$

Equations (18-20) are translated into a d-q reference frame of converter output voltages, rotating at system frequency ω, where a-b-c to d-q transformation matrix is given by *P*.

Defining a state vector as

$$x_i = [i_{1d} \quad i_{1q} \quad i_{2d} \quad i_{2q} \quad v_{cfd} \quad v_{cfq}]^T$$

the state equation in the d-q frame is given by

$$\dot{x}_i = A_i x_i + B_1 u_{dq} + B_2 v_{tdq} \tag{21}$$

Also the control input *u* can be expressed as

$$\begin{aligned} u_{dq} &= -k_1\left(i_{2dq} - i_{2refdq}\right) - k_2\left(i_{1dq} - i_{2dq} - i_{cfrefdq}\right) \\ &\quad - k_3\left(v_{cfdq} - v_{cfrefdq}\right) \\ &= -k_2 i_{1dq} + \left(k_2 - k_1\right) i_{2dq} - k_3 v_{cfdq} + k_1 i_{2refdq} \\ &\quad + k_2 i_{cfrefdq} + k_3 v_{cfrefdq} \end{aligned} \tag{22}$$

The above equation can be written in matrix form as

$$\begin{bmatrix} u_d \\ u_q \end{bmatrix} = G_i x_i + H_i y_{refdq} \tag{23}$$

where

$$y_{refdq} = [i_{2refd} \quad i_{2refq} \quad i_{cfrefd} \quad i_{cfrefq} \quad v_{cfrefd} \quad v_{cfrefq}]^T$$

Substituting (23) into (21) we get

$$\dot{x}_i = \left(A_i + B_1 G_1\right) x_i + B_1 H_i y_{refdq} + B_2 v_{tdq} \tag{24}$$

Since V_{dc} is assumed to be constant, the linearization of (24) will not alter B_1. This linearization results in

$$\Delta\dot{x}_i = A_{CONV}\Delta x_i + B_{CONV}\Delta y_{refdq} + B_2 \Delta v_{tdq} \tag{25}$$

where, $A_{CONV} = A_i + B_1 G_i$ and $B_{CONV} = B_1 H_i$.

The current references can be expressed in terms of the voltage reference and converter model can be expressed as,

$$\Delta\dot{x}_i = A_{CONV}\Delta x_i + B_T \Delta v_{cfrefdq} + B_{BUS}\Delta v_{tdq} \tag{26}$$

where $B_T = B_{CONV}M_1$ and $B_{BUS} = B_{CONV}(M_2 + B_2)$ and the matrices M_1 and M_2 are given in the appendix.

Both the angle and frequency droop controllers are modeled separately from their droop equations (4) and (11) respectively. The droop controller model is then combined with the converter model. All the combined converter and controller models are converted to a common reference frame and then connected to the network to derive the entire microgrid model as shown in [10]. The microgrid model is used to select the parameters of the droop controllers through eigenvalue analysis.

B. Angle Droop and Frequency Droop Controller

With the composite model discussed above, both the droop controllers are designed. The system parameters considered for the study are given in Table-I. The eigenvalue trajectory is plotted by varying either the angle droop or frequency droop gain. The voltage droop gain is held constant. Fig. 4 shows one of the dominant complex conjugate eigenvalue trajectories with the angle droop controller. It can be seen that for a droop controller gain of 0.00045 rad/kW, the complex pole crosses the imaginary axis. Similarly Fig. 5 shows the corresponding eigenvalue trajectory as function of frequency droop controller gain.

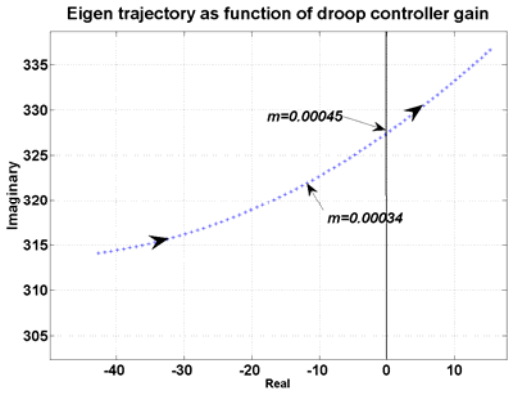

Fig.4. System stability as function of droop gain.

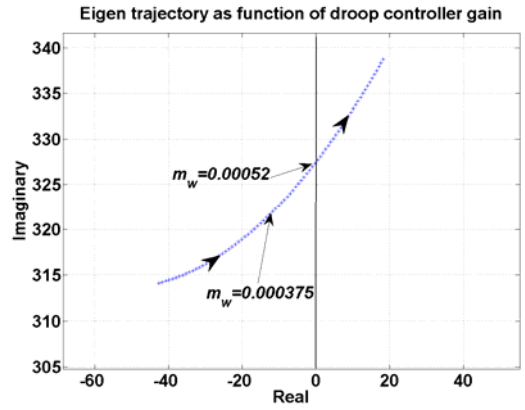

Fig. 5. System stability as function of droop gain.

To compare the results of the two droop controllers, the nominal values of the controller gain are chosen at 75% of the gain at which system becomes unstable. This implies that the

gain with angle droop controller is m = 0.00034 rad/kW and with frequency droop controller is m_ω = 0.000375 rad/s/kW.

V. Simulation Results

Simulations are carried out with both the droop controllers employed separately in the test system shown in Fig. 2. To show the relative differences between the angle and frequency droop controllers, the system condition is kept constant in both the cases.

The output impedances of the two sources are chosen in a ratio of DG-1:DG-2 = 1:1.33 and the power rating of these DGs are also chosen in the ratio of 1.33:1. Same reactive power droop has been used in both the cases. To investigate the frequency deviation, the load conductance is chosen as the integral of a Gaussian white noise with zero mean and a standard deviation of 0.01 Mho. The system parameters and the controller gains are shown in Table-I.

TABLE-I: SYSTEM AND CONTROLLER PARAMETERS

System Quantities	Values
Systems frequency	50 Hz
Load ratings	
Load	2.8 kW to 3.1 kW
DG ratings (nominal)	
DG-1	1.0kW
DG-2	1.33kW
Output inductances	
L_{G1}	75 mH
L_{G2}	56.4 mH
DGs and VSCs	
DC voltages (V_{dc1} to V_{dc4})	0.5kV
Transformer rating	0.415kV/0.415 kV, 0.25 MVA, 2.5% L_f
VSC losses (R_f)	0.1 Ω
Filter capacitance (C_f)	50 μF
Hysteresis constant (h)	10^{-5}
Angle Droop Controller	
m_1	0.000340 rad/kW
m_2	0.000255 rad/kW
Frequency Droop Controller	
m_{w1}	0.000375 rad/s/kW
m_{w2}	0.000281rad/s/kW

Fig. 6 shows the power output of the DGs in case of the angle droop controller. It can be seen that the constant deviation in power output from the DGs are always in the desired ratio and the fluctuation in output power is almost 10% as per the load change.

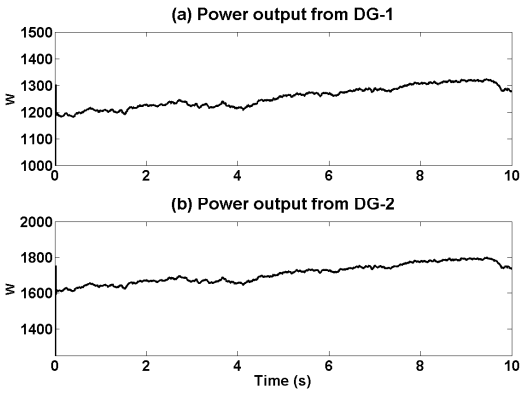

Fig. 6. DG power output with angle droop control.

With the above load fluctuation, the frequency deviation of the DG output in case of angle droop control is shown in Fig. 7. The steady state frequency deviation is zero-mean and the standard deviation of the frequency deviation is 0.01695 rad/s and 0.01705 rad/s respectively for DG-1 and DG-2. The deviation in the frequency is small and the angle droop controller is able to share load in the desired ratio despite the random change in the load demand.

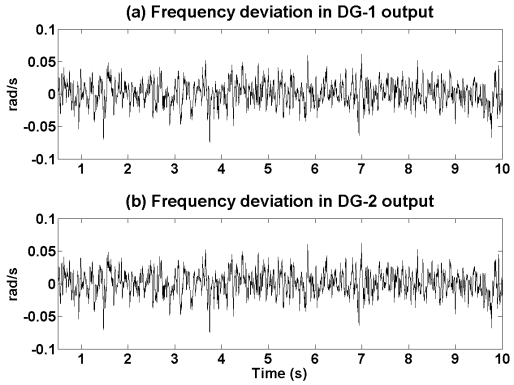

Fig. 7. Frequency variation with angle droop control.

The frequency droop controller is now employed instead of the angle droop. The system is operated under same load fluctuation. The power outputs of the DGs are shown in Fig. 8. It can be seen that the fluctuations in the output powers are much more than the angle droop as shown in Fig. 6.

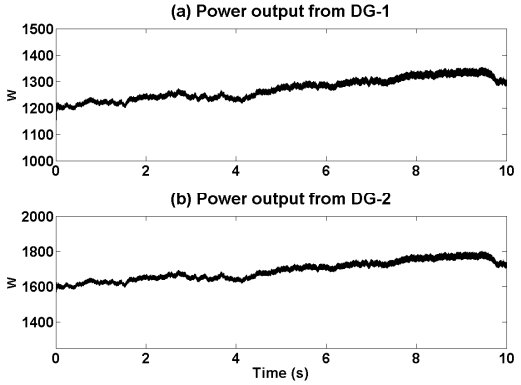

Fig. 8. DG power output with frequency droop control.

The frequency deviation of the DG sources is shown in Fig. 9. It is evident that the frequency variation with the frequency droop controller is significantly higher than that with the angle droop controller.

The standard deviation with the frequency droop controller is 0.4081 rad/s and 0.4082 rad/s respectively for the two DGs. It can also be seen that the mean frequency deviation is much larger in case of frequency droop than in angle droop. This demonstrates that the angle droop controller generates a substantially smaller frequency variation than the conventional frequency droop controller.

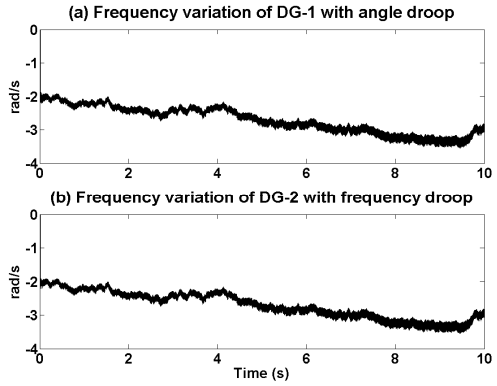

Fig. 9. Frequency variation with frequency droop control

Angle Droop in Multi-DG System:

To investigate the efficacy of the angle droop controller in a microgrid with multiple DGs and loads, angle droop controllers are designed for the system shown in Fig. 10 with system parameter shown in Table-II. It has four DGs and five loads as shown. It is desired that DG-1 to DG-4 share the load in 1.0:2.0:1.5:1.5 ratio. With the system running at steady state, the loads Ld_2 and Ld_3 are disconnected at 0.2 s and the power sharing among the DGs is shown in Fig.11.

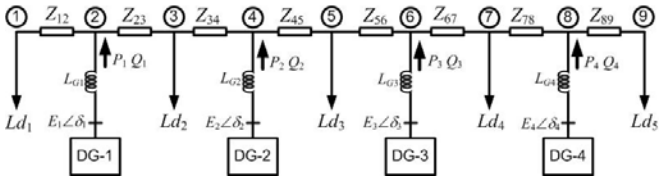

Fig. 10. Microgrid Structure with multiple DGs.

TABLE-II: MICROGRID SYSTEM AND CONTROLLER PARAMETERS

System Quantities	Values
Systems frequency	50 Hz
Feeder impedance $Z_{12} = Z_{23} = Z_{34} = Z_{45} = Z_{45} = Z_{56} = Z_{67} = Z_{78} = Z_{89}$	$0.1 + j\,0.6\ \Omega$
Load ratings	
Ld_1	1.8 kW and 1.6 kVAr
Ld_2	0.8kW and 0.6 kVAr
Ld_3	0.8 kW and 0.6 kVAr
Ld_4	0.8 kW and 0.6 kVAr
Ld_5	1.8 kW and 1.6 kVAr
DG ratings (nominal)	
DG-1	1.0kW
DG-2	2.0kW
DG-3	1.5 kW
DG-4	1.5 kW
Output inductances	
L_{G1}	75 Mh
L_{G2}	37.5 mH
L_{G3}	50 mH
L_{G4}	50mH
DGs and VSCs	
DC voltages (V_{dc1} to V_{dc4})	0.5kV
Transformer rating	0.415kV/0.415 kV, 0.25 MVA, 2.5% L_f
VSC losses (R_f)	0.1 Ω
Filter capacitance (C_f)	50 μF
Hysteresis constant (h)	10^{-5}
Angle Droop Controller	
in multi machine	
m_1	0.1 rad/MW
m_2	0.05 rad/MW
m_3	0.075 rad/MW
m_4	0.075 rad/MW

The efficacy of the angle droop is further verified by sharing power only between DG-1 and DG-4, when DG-2 and DG-3 are disconnected from the system. Let us assume that the system is running in steady state supplying the loads Ld_1, Ld_2 and Ld_4. At 0.2 s, the load Ld_4 is disconnected. The system response is shown in Fig. 12. This test studies the controller response when the power generation and load demand is not evenly distributed along the microgrid. It can be seen that after 0.2 s, the sharing is not very accurate. Choosing a higher droop controller gain, we can assure better sharing in such situations. However, a very high value of droop gain can lead the system to instability as shown in eigenvalue trajectory of Fig. 4. The choice of controller gain is thus a trade off between system stability and system response.

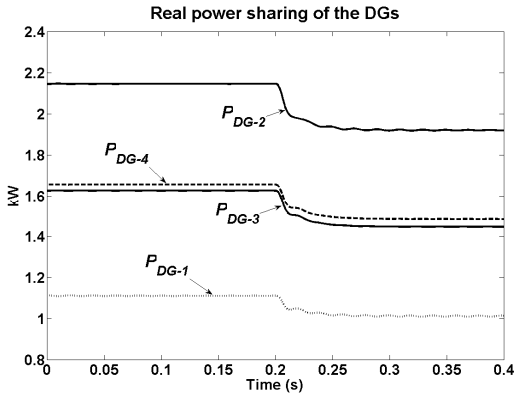

Fig. 11. Real Power Sharing of the DGs.

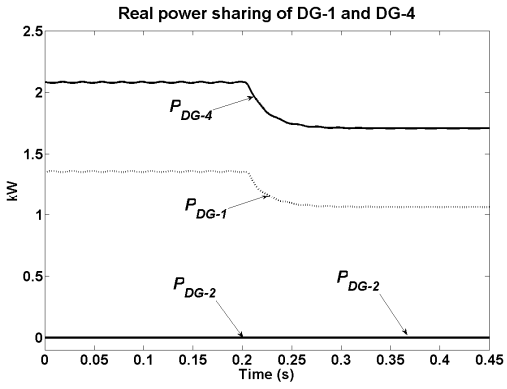

Fig. 12. Real Power Sharing of the DG-1 and DG-4.

VI. CONCLUSIONS

The efficacy of angle droop over frequency droop in a voltage source converter based autonomous microgrid is shown in this paper. The power sharing of the DG sources with angle droop is derived first. A frequency droop controller and an angle droop controller is designed ensuring same stability margin in a two DG system. It is shown that the frequency variation with the frequency droop controller is significantly

higher than that with the angle droop controller. The efficacy of the angle droop controller is further verified in a microgrid with number of DGs and loads.

APPENDIX

The matrices in state space model of a converter are as shown below,

$$P=\frac{2}{3}\begin{bmatrix} \cos(\omega t) & \cos\left(\omega t-\frac{2\pi}{3}\right) & \cos\left(\omega t+\frac{2\pi}{3}\right) \\ -\sin(\omega t) & -\sin\left(\omega t-\frac{2\pi}{3}\right) & -\sin\left(\omega t+\frac{2\pi}{3}\right) \\ \frac{1}{2} & \frac{1}{2} & \frac{1}{2} \end{bmatrix}$$

$$A_i=\begin{bmatrix} -\frac{R_T}{L_T} & \omega & 0 & 0 & -\frac{1}{L_T} & 0 \\ -\omega & -\frac{R_T}{L_T} & 0 & 0 & 0 & -\frac{1}{L_T} \\ 0 & 0 & 0 & \omega & \frac{1}{L_f} & 0 \\ 0 & 0 & -\omega & 0 & 0 & \frac{1}{L_f} \\ \frac{1}{C_f} & 0 & -\frac{1}{C_f} & 0 & 0 & \omega \\ 0 & \frac{1}{C_f} & 0 & -\frac{1}{C_f} & -\omega & 0 \end{bmatrix}$$

$$B_1=\begin{bmatrix} \frac{V_{dc}}{L_T} & 0 \\ 0 & \frac{V_{dc}}{L_T} \\ 0 & 0 \\ 0 & 0 \\ 0 & 0 \\ 0 & \end{bmatrix} \text{ and } B_2=\begin{bmatrix} 0 & 0 \\ 0 & 0 \\ -\frac{1}{L_f} & 0 \\ 0 & -\frac{1}{L_f} \\ 0 & 0 \\ 0 & 0 \end{bmatrix}$$

$$G_i=\begin{bmatrix} -k_2 & 0 & (k_2-k_1) & 0 & -k_3 & 0 \\ 0 & -k_2 & 0 & (k_2-k_1) & 0 & -k_3 \end{bmatrix}$$

$$H_i=\begin{bmatrix} k_1 & 0 & k_2 & 0 & k_3 & 0 \\ 0 & k_1 & 0 & k_2 & 0 & k_3 \end{bmatrix}$$

$$M_1=\begin{bmatrix} 0 & \frac{1}{\omega L_f} \\ -\frac{1}{\omega L_f} & 0 \\ 0 & -\omega C_f \\ \omega C_f & 0 \\ 1 & 0 \\ 0 & 1 \end{bmatrix} \text{ and } M_2=\begin{bmatrix} 0 & -\frac{1}{\omega L_f} \\ \frac{1}{\omega L_f} & 0 \\ 0 & 0 \\ 0 & 0 \\ 0 & 0 \\ 0 & 0 \end{bmatrix}$$

ACKNOWLEDGEMENT

The authors thank the Australian Research Council (ARC) for the financial support for this project through the ARC Discovery Grant DP 0774092.

REFERENCES

[1] F. Katiraei and M. R. Iravani, "Power management strategies for a microgrid with multiple distributed generation units," IEEE Trans. on Power Systems, Vol. 21, No. 4, pp. 1821-1831, 2006.

[2] M. Reza, D. Sudarmadi, F. A. Viawan, W. L. Kling, and L. Van Der Sluis, "Dynamic Stability of Power Systems with Power Electronic Interfaced DG," Power Systems Conference and Exposition, PSCE'06, pp. 1423-1428, 2006.

[3] J. M. Guerrero, L. G. de Vicuna, J. Matas, M. Castilla, and J. Miret, "A wireless controller to enhance dynamic performance of parallel inverters in distributed generation systems," IEEE Trans. on Power Electronics, Vol. 19, No. 5, pp. 1205-1213, 2004.

[4] M. C. Chandorkar, D. M. Divan and R. Adapa, "Control of parallel connected inverters in standalone ac supply systems," IEEE Trans. On Industry Applications, Vol. 29, No. 1, pp. 136-143, 1993.

[5] .M. Reza, D. Sudarmadi, F. A. Viawan, W. L. Kling, and L. Van Der Sluis, "Dynamic Stability of Power Systems with Power Electronic Interfaced DG," Power Systems Conference and Exposition, PSCE'06, pp. 1423-1428, 2006.

[6] D. Pudjianto, G. Strbac, F. Van Overbeeke, A. I. Androutsos, Z. Larrabe, J. Tome Saraiva, "Investigation of Regulatory, Commercial, Economic and Environmental Issues in MicroGrids", Future Power Systems, International Conference on future power system, pp. 1-6, 16-18 Nov. 2005

[7] Digital Control of Dynamic Systems GF Franklin, ML Workman, D Powell - 1997 - Addison-Wesley Longman Publishing Co., Inc. Boston, MA, USA

[8] J. M. Guerrero, L. G. de Vicuna, J. Matas, M. Castilla, and J. Miret, "Droop control method for the parallel operation of online uninterruptible power systems using resistive output impedance,"Applied Power Electronics Conference and Exposition, 2006. APEC '06. Twenty-First Annual IEEE, Page(s):7 pp, 19-23 March 2006.

[9] J. M. Guerrero, L. G. de Vicuna, J. Matas, M. Castilla, and J. Miret, "A wireless controller to enhance dynamic performance of parallel inverters in distributed generation systems," IEEE Trans. on Power Electronics, Vol. 19, No. 5, pp. 1205-1213, 2004.

[10] N. Pogaku, M. Prodanovic, T. C. Green, "Modeling, Analysis and Testing of Autonomous Operation of an Inverter-Based Microgrid," IEEE Trans. on Power Electronics, Vol. 22, Issue-2, pp. 613-625, 2007.

Ritwik Majumder (S'07) received his B.E. in Electrical Engineering from Bengal Engineering College (Deemed University) in 2001 and his M.Sc. (Engg.) degree from Indian Institute of Science in 2004. From July 2004 to November 2004, he was with Tata Motor Engineering Research Centre in Jamshedpur, India. From November, 2004 to January 2006, he was with Siemens Automotive India and from January 2006 to May 2007, he was with ABB Corporate Research Centre, Bangalore, India. Since June 2007, he is a Ph.D. scholar in Queensland University of Technology. His interests are in Power Systems dynamics, Distributed Generation and Power Electronics Applications.

Arindam Ghosh (S'80, M'83, SM'93, F'06) is the Professor of Power Engineering at Queensland University of Technology, Brisbane, Australia. He has obtained a Ph.D. in EE from University of Calgary, Canada in 1983. Prior to joining the QUT in 2006, he was with the Dept. of Electrical Engineering at IIT –Ka npur, India, for 21 years. He is a fellow of Indian National Academy of Engineering (INAE) and IEEE. His interests are in Control of Power Systems and Power Electronic devices.

Gerard Ledwich (M'73, SM'92) received the Ph.D. in electrical engineering from the University of Newcastle, Australia, in 1976. He has been Chair Professor in Power Engineering at Queensland University of Technology, Australia since 2006. Previously he was the Chair in Electrical Asset Management from 1998 to 2005 at the same university. He was Head of Electrical Engineering at the University of Newcastle from 1997 to 1998. Previously he was associated with the University of Queensland from 1976 to 1994. His interests are in the areas of power systems, power electronics, and controls. He is a Fellow of I.E.Aust.

Dr Firuz Zare (M'97, SM'06) was born in Iran in 1967. He holds a PhD degree in Electrical Engineering from Queensland University of Technology in Australia. He has worked as a development engineer and a consultant in industry for several years. He has joined the school of engineering systems in QUT in 2006. His research interests are power electronic applications, pulse-width modulation techniques, renewable energy systems and electromagnetic interferences.